Predicting tearing paths in thin sheets

A. Ibarra,[1] J. F. Fuentealba,[1,*] B. Roman,[2] and F. Melo[1]
[1]*Departamento de Física Universidad de Santiago de Chile, Avenida Ecuador 3493, 9170124 Estación Central, Santiago, Chile*
[2]*PMMH, ESPCI Paris, PSL Research University, CNRS UMR7636, Sorbonne Université, Université de Paris, 10 rue Vauquelin 75005, Paris, France*

(Received 27 February 2019; published 8 August 2019)

This study investigates the tearing of a thin notched sheet when two points on the sheet are pulled apart. The concepts that determine the crack trajectory are reviewed in the general anisotropic case, in which the energy of the fracture depends on the fracture direction. When observed as a flat sheet a purely geometric "tearing vector" is defined through the location of the crack tip and the pulling points. Both Griffiths's criterion and the maximum energy release rate criterion (MERR) predict a fracture path that is parallel to the tearing vector in the isotropic case. However, for the anisotropic case, the application of the MERR leads to a crack path that deviates from the tearing vector, following a propagation direction that tends to minimize the fracture energy. In the case of strong anisotropy, it is more difficult to obtain an analytical prediction of the tearing trajectory. Thus, simple geometrical arguments are provided to give a derivation of a differential equation accounting for crack trajectory, according to the natural coordinates of the pulling, and in the case that the anisotropy is sufficiently weak. The solution derived from this analysis is in good agreement with previous experimental observations.

DOI: 10.1103/PhysRevE.100.023002

I. INTRODUCTION

The prevention of crack nucleation is a key objective in the engineering and design of reliable structures [1–3]. However, predicting and controlling the crack pathway also has important applications, such as the design of easy to tear packaging [4,5] or fracture-induced patterning on a micro- [6] or nanoscale [7]. Additionally, in order to further the design of tough materials, printing materials with patterns composed of precut segments and sacrificial zones favor the development of a desired crack path to enable predictable and progressive fracture propagation [8].

In applications such as packaging, fracture propagation is desirable, and the control of the pathway of the crack trajectory is highly beneficial. For instance, spiral tearing has been suggested as an elegant way for the fast and efficient unwrapping of a present [5]. However, achieving the appropriate tear control is often hindered by the complex nature of the material in question and an insufficient understanding of the physical laws of fracture propagation involving large sheet deflections. Indeed, both stress distribution and fracture head shape are determined by the properties of local materials, such as plasticity, anisotropy and texture. In turn, common experience indicates that the geometrical properties of the points over which forces are applied, and the corresponding pulling directions, are the fundamental parameters controlling fracture path and the mechanical work to sustain tearing progression.

Pioneering work by O'Keefe [9] investigated how a piece of paper tears when simultaneously pulled apart by two points. O'Keefe's experimental setup includes a notch being cut into a brittle thin sheet and the selection of two points, A and B, on either side of the notch. Subsequently, these two points are pulled apart, applying only forces (no torque) (see Fig. 1). This study enabled the identification of geometric and energetic aspects of the tearing problem and introduced for the first time the role of fracture-energy anisotropy [9], which is closely related to the oriented fibered structure of ordinary paper. It is crucial to consider the anisotropy of fracture energy, as in nature materials with anisotropic fracture energy occur more frequently compared to isotropic ones. In addition, the latter are very difficult to manufacture.

Although O'Keefe's work was enlightening, it was not based on the principles of fracture mechanics, thus leading to inaccurate and intricate variable relations for crack trajectories. This article predicts theoretically the crack trajectory in a strongly deformed brittle sheet, with a tearing configuration of two points being pulled apart. Fracture propagation is modeled within the inextensible framework [10], where the energy release rate is linear to the applied force [11,12], unlike in linear elastic fracture mechanics [13]. In general, the fracture path is considered, and in the case of weak fracture anisotropy an analytical expression is derived.

In a previous work, experiments are carried out with bioriented polypropylene sheets. These are much more homogeneous than paper and give a perfectly smooth fracture path [12]. These sheets have a weakly anisotropic fracture energy with two orthogonal principal axis of symmetry. It was observed that the trajectories are reproducible and that the propagation direction depends solely on the position of the crack's tip and is independent of the past propagation [12]. As a result, all experimental tearing pathways are related and have nonintersecting trajectories (see Fig. 2). In addition, these trajectories tend to deflect and curve away from the furthest pulling point. The trajectories that are most similar to a straight line correspond to cases where the fracture tip C is

*juan.fuentealbadu@usach.cl

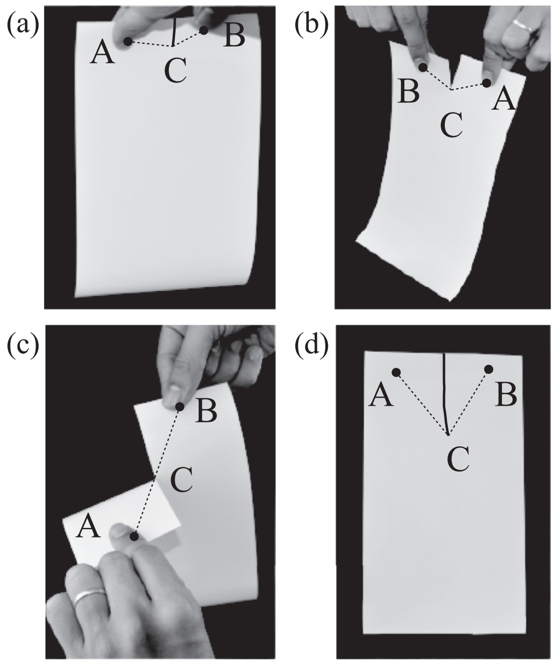

FIG. 1. Photos demonstrating the tearing of paper by hand. (a) Two pulling points are selected, A and B, and a notch is made between these two points until point C. (b) Points A and B are gradually pulled apart. Straight lines demonstrate the relation between the pulling points and the head of the crack or tear. (c) If the sheet is thin and flexible enough, points A (and B) become aligned in a single straight line, and a fracture propagates when there is a strong enough pulling force. (d) It is assumed that the sheet cannot be extended. Thus, in order to investigate the geometrical features of tearing, the sheet should be observed on a flat surface or "flat representation."

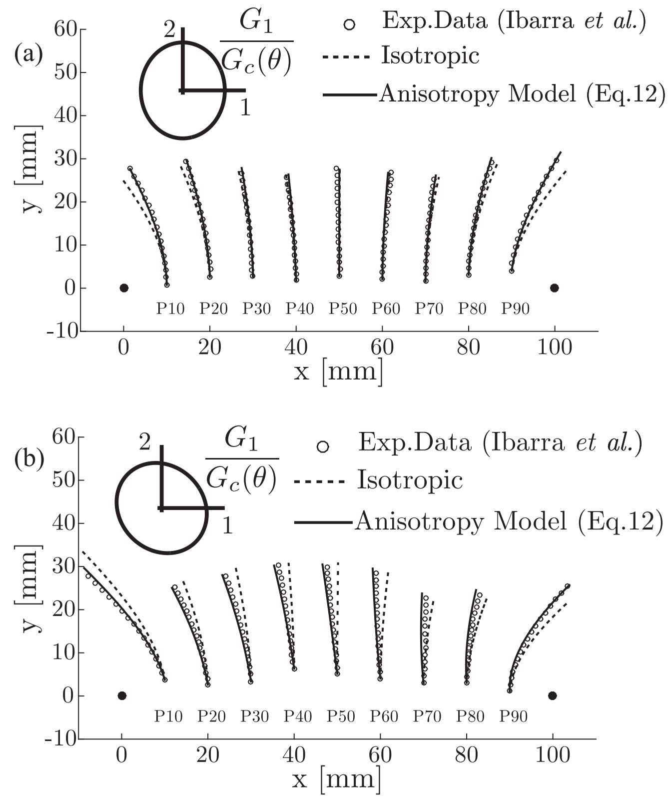

FIG. 2. Observed fracture trajectories as presented by Ibarra *et al.* [12] for various locations of the initial crack, with a constant pulling speed and two orientations of symmetry axis 1 with respect to the focal axis, compared to the theoretical predictions within this study. The line joining the pulling points (located 100 mm apart and indicated by black dots) indicates the focal axis. (a) Symmetry axis 1 oriented parallel to focal point axis, $\theta_0 = 0$. (b) Symmetry axis 1 oriented at $\theta_0 = \pi/4$ with respect to the focal axis. Insets to the left indicate the orientation of the symmetry axis of fracture energy. Note that $G_1/G_c(\theta)$ is indicated for greater clarity.

at equal distance from both pulling points. Furthermore, it was noted that the trajectories differ depending on the orientation of the sheet, which highlights the role of the anisotropy of the sheet [compare Figs. 2(a) and 2(b)].

Material anisotropy is presented in a general and systematic manner based on a Wulff's type diagram [14], providing the propagation direction in a scenario where the crack tip position is known. Through a recursive application of the Wulff's type diagram, the experimental crack trajectory is predicted in the general case of two pulling points, and a good prediction is made of the applied force that leads to tearing, without making any adjustments of parameters [12]. However, this approach does not give an analytical derivation of the crack trajectories.

Here the mechanical principles of fracture propagation in thin films are investigated, and it is shown how to derive rigorously analytical predictions of crack pathways using these principles along with a simple hypothesis [10,12]. This approach towards deriving differential equations of crack pathways is based on the fact that, when a material is isotropic, the fracture follows a perfect hyperbola. Small deviations from hyperbolas, induced by the material anisotropy, are well described by a differential equation represented in this natural hyperbolic coordinates system. Theoretical trajectories compare very well with the previously reported experimental results [12], without adjusting the parameters.

II. GENERAL FRACTURE CRITERION

A. Fracture criterion in isotropic materials

The classical Griffith criterion establishes that a crack can propagate in a generic direction θ if the energy released per unit of fracture surface, $G(\theta)$, compensates for the energy cost of fracturing the material $G_c(\theta)$, so that $G(\theta) = G_c(\theta)$. This criterion expresses energy conservation, therefore it is always valid, but an additional criterion is required to determine propagation direction. A widely accepted criterion is to assume that a fracture propagates in the direction that maximizes the energy release rate. This maximum energy release rate (MERR) criterion is equivalent to the principle of local symmetry for continuous trajectories [15,16] and is valid for smooth propagation in isotropic materials.

The calculation of the energy release rate $G(\theta)$ is given for the tearing configuration in Fig. 1. In order to visualize the geometrics of pulling, the sheet should first be investigated during tearing. An important observation made during the experiment was that the two lines (AC, BC) marked on the sheet, which join the pulling points to the crack tip C, become a single straight line during the application of force [see Fig. 3(a)].

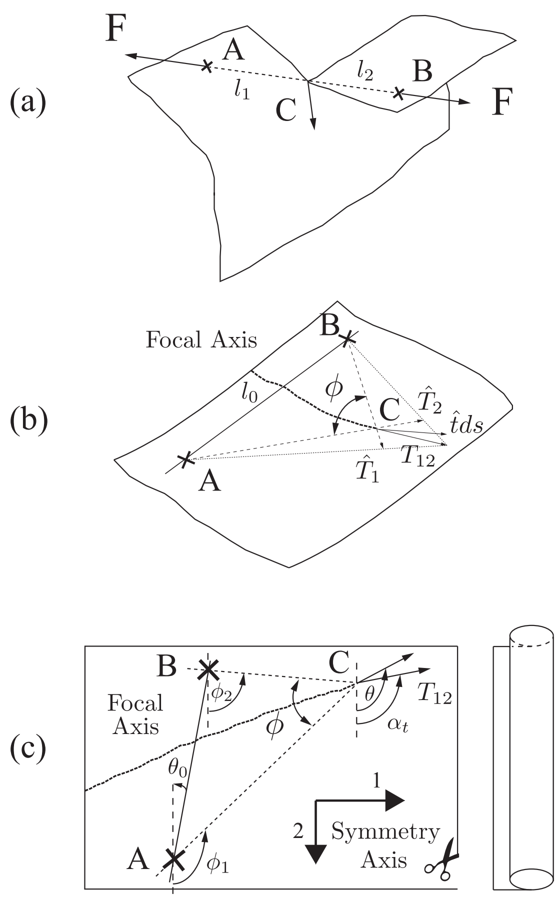

FIG. 3. (a) A three-dimensional diagram presenting tearing by pulling of two points. (b) Diagram illustrating the identified geometrical variables and vectors with respect to a flat sheet. (c) On the sheet, the reference orientation is identified to be along the major axis of symmetry of the fracture energy, axis 1. The orientation of axis 1 with respect to the axis joining the pulling points, or the focal axis, is θ_0.

This occurs because the sheet is extremely bendable and is unable to sustain torques. Additionally, it is observed that the application of force on a thin, inextensible sheet means that no stretching energy is stored within the sheet. Thus, the energy release rate corresponds exactly to the work carried out by the operator per unit of surface created, $G(\theta)hds = F dl_T$, where h is the sheet thickness, F is the force applied as the crack advances by ds, and $dl_T = dl_1 + dl_2$ is the total distance increase between the pulling points (along the pulling direction), where $l_1 =$ distance AC and $l_2 =$ distance BC. The crack trajectory in the flat sheet can be examined where l_0 represents the length of segment AB [Fig. 3(b)]. In this case the distances will not be modified because the sheet is almost inextensible. The following dimensionless unit vectors are defined as $\hat{T}_1$ and $\hat{T}_2$, joining the fracture tip to the pulling points, with the sheet observed as a flat surface [Fig. 3(b)]. As the fracture advances by a distance of ds in the direction $\hat{t}$, the following is observed: $dl_1 = \hat{T}_1 \cdot \hat{t} ds$ and $dl_2 = \hat{T}_2 \cdot \hat{t} ds$, giving the energy release rate

$$G(\theta)h = F(\hat{T}_1 + \hat{T}_2) \cdot \hat{t}. \quad (1)$$

In the case that the fracture energy is isotropic, the energy release rate is maximized when the fracture direction $\hat{t}$ is parallel to the tearing vector, defined as $\vec{T}_{12} = \hat{T}_1 + \hat{T}_2$. Considering that the tearing vector bisects the lines joining the pulling points to the fracture tip, the crack trajectories are therefore portions of hyperbolas, with the pulling points as their focal points. This is consistent with the trajectories observed in Fig. 2. These appear to curve away from the closest pulling point and tend to present themselves as straight asymptotes remotely positioned from the focal points, as expected for hyperbolas. However, comparisons between experiments with theoretical predictions (presented as dashed lines in Fig. 2) indicate systematic deviations from the hyperbolic pathways predicted for isotropic sheets. Thus, herein the effect of material anisotropy is investigated.

B. Fracture criterion in anisotropic materials

In the case of an anisotropic material, a simple and natural generalization is given of the MERR criterion [12] to define the direction of propagation. Indeed, assuming that loading progressively increases, it is suggested that that fracture propagates in the initial direction that fulfills Griffith's criterion [16–20]. Thus, cracks propagate in the direction θ, such that

$$G(\theta) = G_c(\theta), \quad (2)$$

$$\frac{dG(\theta)}{d\theta} = \frac{dG_c(\theta)}{d\theta}. \quad (3)$$

As a general rule, in the presence of anisotropy a crack will not propagate in the direction of the maximum energy release; instead it will be deflected towards a direction with lower fracture energy. This condition [Eq. (3)] is also referred to as an Eshelby torque (to the left-hand side), corresponding to a material torque associated with anisotropy in fracture energy [18]. Although this criterion [Eqs. (2) and (3)] was put forward during the 1970s [17], and supported by the numerical phase field approach [18–20], only recently was it tested under experimental conditions using the specific geometry of the tearing direction of a anisotropic film in a simplified and symmetric configuration [12,14].

Also, it was demonstrated that the tangency condition together with the Griffith criterion led to a generalized form of Wulff's construction [14], enabling the prediction of crack direction and pulling force by inputting the fracture energy G_c as a function of propagation angle. The experimental results from the trousers test configuration are in good agreement with previous predictions [14]. More recently, it was demonstrated that under these fracture propagation conditions it is possible to accurately predict the crack direction for the general case of pulling apart two points [12]. Subsequently, a different approach is adopted [12] to find a differential equation that accounts for fracture propagation.

When two points are pulled apart, the angular dependence of the energy release rate is explained in Eq. (1) leading to

$$G(\theta)h = 2F \cos(\phi/2)\cos(\theta - \alpha_t),$$

where θ and α_t are, respectively, the propagation angle and the angle of the tearing vector $\vec{T}_{12}$, with respect to a reference axis in the sheet [see Fig. 3(c)], and ϕ is the angle ACB. Griffith's criterion (2) now becomes

$$2F\cos\left(\frac{\phi}{2}\right)\cos(\theta-\alpha_t)=G_c(\theta)h. \tag{4}$$

The Eshelby condition (3) then reads

$$-2F\cos\left(\frac{\phi}{2}\right)\sin(\theta-\alpha_t)=\frac{dG_c(\theta)}{d\theta}h. \tag{5}$$

These two equations (4) and (5) are unspecific. However, it is noted that the energy release rate $G(\theta)$ takes on a very simplified form, as seen in Eq. (1). In particular $G(\theta)$ does not depend on the properties of the elastic material, which are most certainly anisotropic. This greatly simplifies the problem, as only anisotropy should be considered in the description of fracture energy.

Equations (4) and (5) then lead to

$$\tan(\theta-\alpha_t)=-\frac{dG_c(\theta)}{d\theta}\frac{1}{G_c(\theta)}. \tag{6}$$

Thus, given the fracture energy G_c and the direction of the tearing vector α_t, it is possible to determine the propagation angle θ. It should be noted that if the material is isotropic, propagation occurs along the tearing vector, since $\theta=\alpha_t$. The tearing angle, α_t, is a function of the location of the pulling points with respect to the crack tip. In general, the implicit relation [Eq. (6)] is not simple to use. Therefore, a graphical construction is proposed, which is often used under the discipline related to crystal growth, as described in previous studies [12,14].

C. The vanishing anisotropy limit approximation for crack trajectories

The previous equations predict the crack direction for any anisotropic fracture energy. However, the differential equation followed by the crack path and the possible solutions of such an equation remain unresolved. This study partially elucidates these unknown aspects through the limit of small anisotropy using the variables l_1-l_2 and l_1+l_2. It is noted that in the case of null anisotropy any possible crack path is characterized by l_1-l_2, equal to a constant ($dl_1=dl_2$, hyperbolic trajectories). The natural orthogonal coordinate of l_1-l_2 is l_2+l_1, thus the differential equation for the isotropic case is, $d(l_1-l_2)/d(l_1+l_2)=0$. As seen from Eq, (6), with the effect of anisotropy slightly modifying hyperbolic trajectories, consequently the following equation is determined: $d(l_1-l_2)/d(l_1+l_2)\ll 1$.

Geometrically, the vector $\hat{t}$ tangent to the crack trajectory can be written as

$$\hat{t}=\frac{\hat{T}_1+\hat{T}_2}{|\hat{T}_1+\hat{T}_2|}\cos(\theta-\alpha_t)+\frac{\hat{T}_1-\hat{T}_2}{|\hat{T}_1-\hat{T}_2|}\sin(\theta-\alpha_t). \tag{7}$$

Since $dl_1=\hat{t}\cdot\hat{T}_1ds$ and $dl_2=\hat{t}\cdot\hat{T}_2ds$, the above expression can be used to calculate $d(l_1-l_2)$ and $d(l_1+l_2)$, giving

$$\frac{d(l_1-l_2)}{d(l_1+l_2)}=\tan(\phi/2)\tan(\theta-\alpha_t)=-\tan(\phi/2)\frac{G_c'(\theta)}{G_c(\theta)}. \tag{8}$$

The term in the product can be expressed as $\tan(\phi/2)=\sqrt{\frac{l_0^2-(l_1-l_2)^2}{(l_1+l_2)^2-l_0^2}}$, while an explicit expression of $G_c(\theta)$ is needed to achieve further progress. For such purposes, we choose to use a general expression of $G_c(\theta)$, validated recently for oriented polypropylene sheets by Ibarra *et al.* [12], $G_c(\theta)=G_1\cos^2\theta+G_2\sin^2\theta$. Since the observed anisotropy in this material is small, we then define $\Delta G_c\equiv G_1-G_2\ll G_1$, which leads to

$$\left.\frac{G_c'(\theta)}{G_c(\theta)}\right|_{\alpha_t}\approx\frac{2\Delta G_c\sin(2\alpha_t)}{G_0}, \tag{9}$$

where $G_0=(G_1+G_2)/2$. In order to simplify the calculation, one of the symmetry axes is considered parallel to the focal axis, $\theta_0=0$, with θ_0 the angle made by the symmetry and the focal axis [Fig. 3(c)]. The relevant trigonometric functions of α_t are expressed in terms of l_1-l_2 and l_1+l_2. Initially the following is observed [Fig. 3(c)]: $2\alpha_t=\phi_1+\phi_2$. By using $\sin(2\alpha_t)=\sin(\phi_1)\cos(\phi_2)+\sin(\phi_2)\cos(\phi_1)$ and geometrical relations, the following is obtained: $l_0\sin(\phi_1)=l_2\sin(\phi)$ and $l_0\sin(\phi_2)=l_1\sin(\phi)$ and through the cosines theorem, $\cos(\phi_1)=\frac{l_1^2-l_2^2+l_0^2}{2l_0l_1}$ and $\cos(\phi_2)=\frac{l_1^2-l_2^2-l_0^2}{2l_0l_2}$, which finally

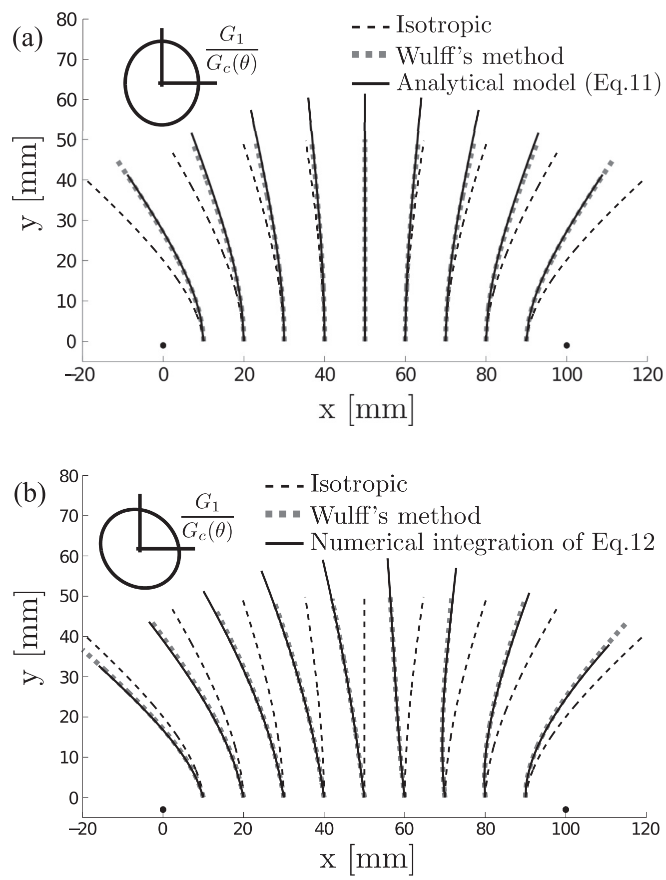

FIG. 4. (a) Estimated crack trajectories obtained from Eq. (11), for $\theta_0=0$, compared to the exact solution predicted using Wulff's method presented in Ref. [12]. (b) Estimated crack trajectories obtained from the numerical solution of Eq. (12) compared to Wulff's solution [12] for $\theta_0=\pi/4$. Isotropic solutions are included in panels (a) and (b) so they can be compared.

leads to

$$\frac{du}{dv} = \frac{\Delta G}{G_0}\left[\frac{2uv}{l_0^2}\frac{u^2 - l_0^2}{v^2 - u^2}\right], \tag{10}$$

where $u = l_1 - l_2$ and $v = l_1 + l_2$. In order to solve this equation, u is replaced by its initial value in the denominator of the right-hand term, which is justified since v varies more rapidly than u (u is constant in the isotropic case). Integration leads to

$$u \approx \frac{\Delta G}{G_0}\left[\left(\frac{u_0}{l_0}\right)^2 - 1\right] u_0 \ln\left(\frac{v^2 - u_0^2}{v_0^2 - u_0^2}\right) + u_0. \tag{11}$$

For any orientation θ_0 of the symmetry axis, the general equation for the crack trajectories is

$$\frac{du}{dv} = \frac{\Delta G}{G_0}\left[2\frac{uv}{l_0^2}\frac{u^2 - l_0^2}{v^2 - u^2}\cos(2\theta_0) + \sqrt{\frac{l_0^2 - u^2}{v^2 - l_0^2}} \times \left\{\frac{v^2 + u^2 - 2u^2v^2/l_0^2}{v^2 - u^2}\right\}\sin(2\theta_0)\right]. \tag{12}$$

In order to validate these analytical approximations, the trajectories given by the geometrical Wulff's construction, obtained by Ibarra *et al.* [12], are compared. In the case of $\theta_0 = 0$ and $\theta_0 = \pi/4$ the analytical solution [Eq. (11)] is an optimal approximation to the crack trajectories [Fig. 4(a)]. For intermediate cases, the solution of Eq. (12) can be obtained numerically. This agrees well with the exact solution from Wulff's method [12] [Fig. 4(b)].

It is worth mentioning that in practical situations Eq. (11) allows for a direct estimation of the fracture energy anisotropy $\Delta G/G_0$. This is realized by measuring the corresponding distance between pulling points (l_0) on the sheet and the initial location of the crack tip (u_0, v_0) and from the torn sheet the pair (u, v) on the crack trajectory. If the fracture advances a significant distance, in practice $v - v_0$ is of the order of l_0, then $\Delta G/G_0$ can be deduced from Eq. (11) with about 10% uncertainty.

III. CONCLUSIONS

This article focuses on the simplest tearing configuration where two arbitrary material points on the sheet are pulled apart from the crack tip. During fracture, the thin sheet undergoes high levels of out-of-plane deformation. However, assuming that the sheet is inextensible and infinitely bendable, a simple representation of the highly bent sheet into a flat sheet facilitates the calculation of the energy release rate $G(\theta)$ for any propagation direction θ through an energetic approach.

This is attained through the identification of an effective pulling vector, which is easily calculated for any geometrical configuration. Thus, this is a simple approach to introduce fracture physics and calculate fracture trajectories. In the case of isotropic materials, fracture trajectories are expected to be perfect hyperbolas with focal points that are defined by the pulling points. However, in the presence of anisotropy, the fracture is deflected towards directions with less fracture energy, which is consistent with the tangency condition of $G(\theta)$ and $G_c(\theta)$ curves, which maximize the ratio $G(\theta)/G_c(\theta)$. Exploring these conditions within the natural variables of the problem, the hyperbolic coordinates give differential equation that, given the pulling points and the initial notch location, gives predictions of the tearing trajectories. For a slight anisotropy regime, this prediction is in good agreement with experiments under similar conditions, without adjustable parameters.

ACKNOWLEDGMENTS

The authors are very grateful to José Bico for enlightening discussions. We acknowledge the support from the Convenio de Desempeño USA1799 of Universidad de Santiago de Chile, Fondecyt Grant No. 1161010, Fondecyt Grants No. 3170907 and No. Anillo 1412. The Laboratoire International Associé "Matière: Structure et Dynamique," LIA-MSD, is kindly acknowledged for supporting this scientific collaboration.

[1] R. R. Meehan and S. J. Burns, Exp. Mech. **38**, 103 (1998).
[2] R. S. Rivlin, Paint Technol. **9**, 215 (1944).
[3] J. W. Hutchinson and Z. Suo, Adv. Appl. Mech. **29**, 63 (1992).
[4] J.-F. Fuentealba, E. Hamm, and B. Roman, Phys. Rev. Lett. **116**, 165501 (2016).
[5] V. Romero, B. Roman, E. Hamm, and E. Cerda, Soft Matter **9**, 8282 (2013).
[6] K. H. Nam, I. H. Park, and S. H. Ko, Nature (London) **485**, 221 (2012).
[7] L. F. Pease, P. Deshpande, Y. Wang, W. B. Russel, and S. Y. Chou, Nat. Nanotech. **2**, 545 (2007).
[8] M. Mirkhalaf, A. Khayer Dastjerdi, and F. Barthelat, Nat. Commun **5**, 3166 (2014).
[9] R. O'Keefe, Am. J. Phys. **62**, 299 (1994).
[10] B. Roman, Int. J. Fract. **182**, 209 (2013).
[11] T. Wierzbicki, K. A. Trauth, and A. G. Atkins, J. Appl. Mech. **65**, 990 (1998).
[12] A. Ibarra, B. Roman, and F. Melo, Soft Matter **12**, 5979 (2016).
[13] B. Lawn, *Fracture of Brittle Solids*, 2nd ed., Cambridge Solid State Science Series (Cambridge University Press, Cambridge, 1993).
[14] A. Takei, B. Roman, J. Bico, E. Hamm, and F. Melo, Phys. Rev. Lett. **110**, 144301 (2013).
[15] M. Amestoy and J.-B. Leblond, Int. J. Solids Struct. **29**, 465 (1992).
[16] A. Chambolle, G. Francfort, and J.-J. Marigo, J. Mech. Phys. Solids **57**, 1614 (2009).
[17] K. Palaniswamy and W. G. Knauss, in *Mechanics Today*, edited by S. Nemat-Nasser (Pergamon Press, New York, 1978), Vol. 4, pp. 87–148.
[18] V. Hakim and A. Karma, J. Mech. Phys. Solids **57**, 342 (2009).
[19] V. Hakim and A. Karma, Phys. Rev. Lett. **95**, 235501 (2005).
[20] B. Li, C. Peco, D. Millán, I. Arias, and M. Arroyo, Int. J. Numer. Meth. Eng. **102**, 711 (2015).